Coordinated by Guillaume Cambois

Near-surface, *SH*-wave surveys in unconsolidated, alluvial sediments

ROGER A. YOUNG, *University of Oklahoma, Norman, U.S.*
JORGE HOYOS, *Manizales, Colombia*

The past decade of hydrocarbon exploration has been marked by sweeping technological innovations that have greatly advanced methods for exploration and development of oil and gas reserves. An example of major importance is the use of shear waves in marine oil and gas exploration to image reflectors beneath gas chimneys. This technology grew from infancy to maturity in the 1990s, is now incorporated into commercial processing packages, and is being used with success in a number of situations. Recent SEG Annual Meetings and the Special Section of this issue of *TLE* have had many documented case histories about the use of converted (*P-SV*) waves.

The *SH*-wave (another type of shear wave), however, has been of less interest to the energy industry during the past decade. Near-surface applications of *SH*-waves, in contrast, have received increasing attention. The present article briefly reviews shear-wave technology advances made in the energy industry over the past decade that prepared the way for the present near-surface application of *SH*-waves. The article concludes with a near-surface case study using combined *P*- and *SH*-wave interpretation in an unconsolidated, alluvial setting.

What are *SV*- and *SH*-waves? A shear wave having particle motion in a horizontal direction is called an *SH*-wave. It stands in contrast to an *SV*-wave, for which particle motion is in the vertical plane. *SH*-waves travel the entire path from source to receiver as shear waves, but recorded *SV*-waves commonly start as *P*-waves at the source and are converted to *SV*-waves by reflection along the way.

SH-waves had their energy industry heyday in the late 1980s and early 1990s after an extensive field study directed by Conoco (the Conoco Group Shoot) and supported by many oil companies (Domenico and Danbom, 1987). That study spurred interest in the imaging potential of shear waves. Tatham and McCormack (1991) suggested a comparison of *P* and *SH* interval traveltimes to determine V_P/V_S ratios. Garotta (1987) was an early advocate of combined interpretation of *P-P* and *P-SV* converted-wave reflections generated by a compressional source and recorded on biphones (radial and vertical sensitivity). The prospect of shear-wave imaging motivated the development of multidirectional sources that generated *P*-, *SH*-, and *SV*-wave polarizations. Multicomponent geophones with a 54° design used in VSP surveys (Gal'perin, 1974) were added to the conventional vertical/radial/transverse triad for surface recording. Software algorithms were developed to extract any wave polarization from the resulting multidirectional source/multicomponent receiver records (Alford, 1986).

The rapid growth in 3-D marine exploration seismology from 1985 to 1990, however, eclipsed the acquisition of multicomponent data on land. Although three-component land data were used to map fracture sets from surface data (e.g., Lynn et al., 1996) and in the borehole (e.g., MacBeth, 1996) during the 1990s, the decade was characterized more by development of converted-wave methods

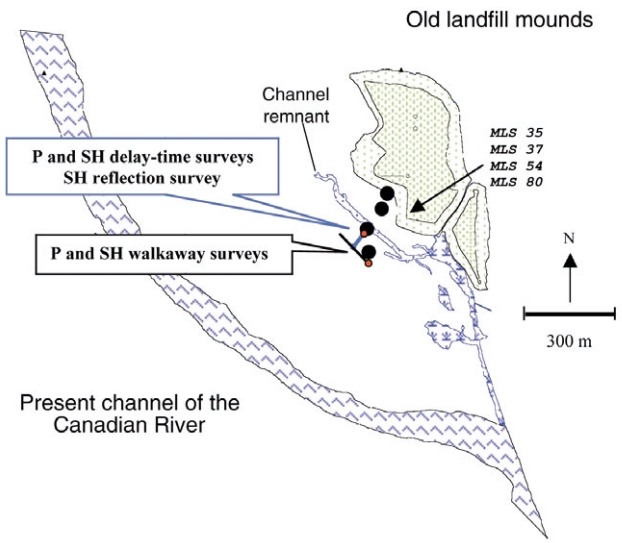

Figure 1. The study area is at the edge of an old landfill in Norman, Oklahoma. Locations of surveys are lines marked by starting points (red). Boreholes (black) were instrumented with multilevel water samplers and were used for stratigraphic and hydrologic control. Landfill mounds (green) are upgradient from the present Canadian River channel (blue). (Map after Scholl and Christenson, 1998.)

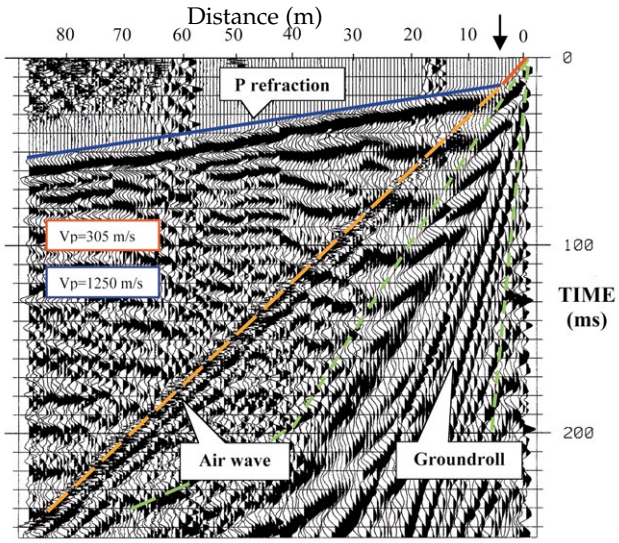

Figure 2. A single *P*-wave refraction (blue) has a crossover at a short distance (black arrow) from the source and persists across the entire record. A high-frequency air wave (dashed orange) coincides with the direct arrival (red) at short distances. Apparent velocities are given in boxes. *P*-wave reflections occurring at early times will be overprinted by a strong, dispersive, ground-roll train (dashed green envelope).

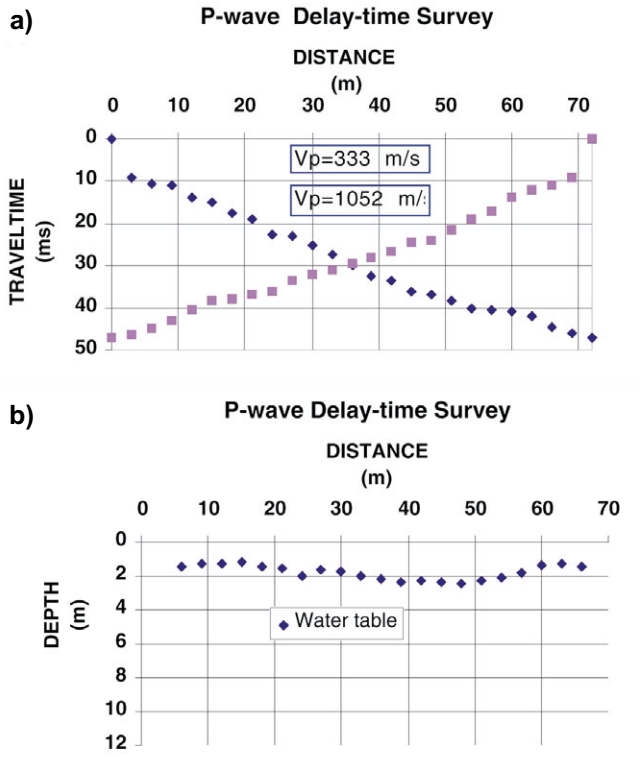

Figure 3. (a) Forward and reversed *P*-wave refraction arrivals are mapped (b) to their corresponding water table refractor depths. The apparent fluctuation in depth to the refractor is due largely to the variation in *P*-wave velocity above the water table, which has not been considered in converting to depth. *P*-wave velocities of the dry and saturated alluvium are 333 and 1052 ms, respectively.

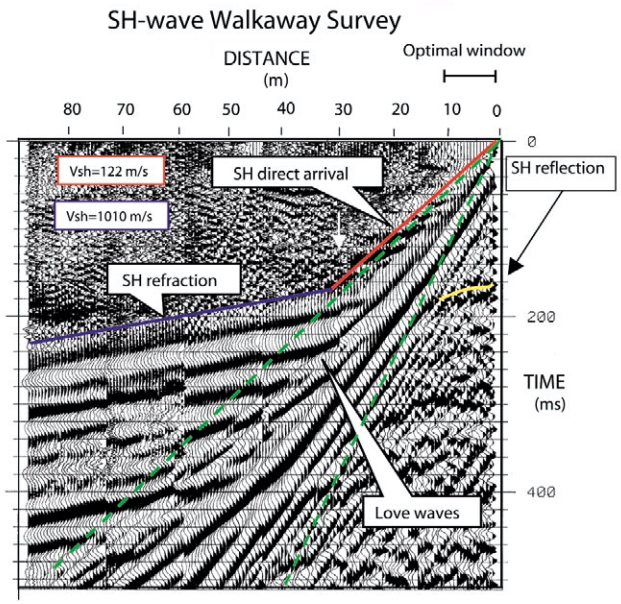

Figure 4. The *SH*-wave refraction (blue) crossover point (white arrow) with the direct arrival (red) occurs at a much greater distance than in the *P*-wave case (Figure 2). Apparent velocities are given in boxes. The dispersive Love waves (dashed green envelope) do not interfere with a shallow, *SH* reflection (yellow) in the optimal window.

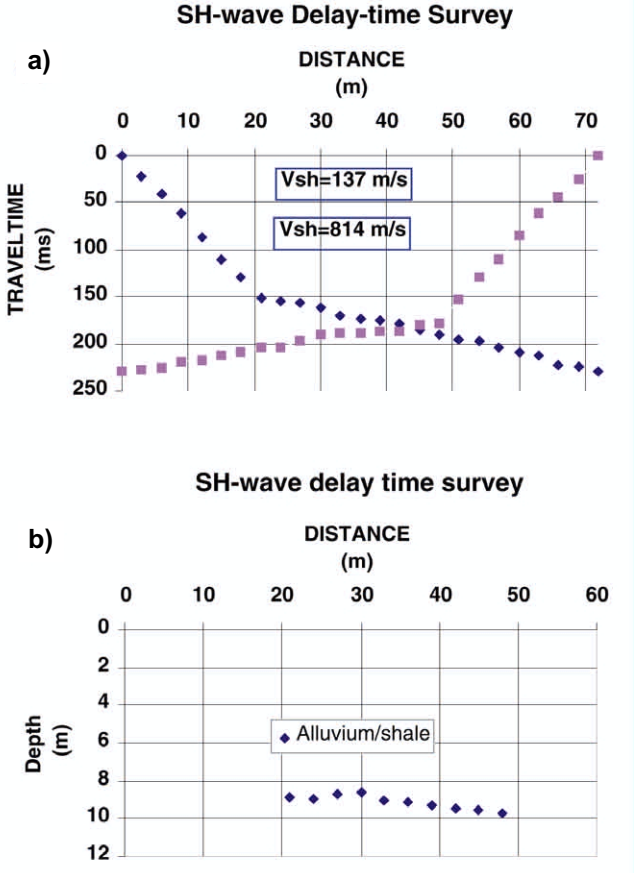

Figure 5. (a) Forward and reversed *SH*-wave refraction arrivals are mapped (b) to their correponding refractor depths at the top of the Hennessey shale. Velocities of the alluvium and shale are 137 and 814 m/s, respectively.

Figure 6. *SH*-wave CMP survey at the Norman landfill. Transverse component geophones (yellow) at .3 m (1 ft) intervals recorded a single transverse hammer blow on the Hasbrouck "golfshoe." A completed, multilevel sampling well (yellow tower) provided lithology constraints for interpretation.

by the CREWES Project at the University of Calgary, for example, as well as by other academic and industry groups. In the last several years, a number of multicomponent land 3-D surveys have been reported (e.g., Simmons et al.,1999; Macrides and Kelamis, 2000), but the focus is still on *SV*-wave applications more often than on *SH*.

Near-surface application of SH-wave surveys. While *SH*-wave applications languished in the energy industry in the 1990s, the near-surface seismic exploration community was putting *SH*-waves to use in high-resolution imaging of targets at depths of less than 100 m. The choice of *SH*-wave rather than *P*-wave surveys contributed to successful imaging in a number of sedimentary environments (e.g., Hasbrouck, 1991; Goforth and Hayward, 1992; Alvarez et al., 1995; Robertsson, et al., 1996; Carr et al., 1998). The suitability of inexpensive *SH*-wave sources, the availability of

horizontal component geophones, the adequacy of short spread lengths attainable with small systems, and the ability to process *SH* surveys with inexpensive reflection software packages all have contributed to the near-surface community's increased activity in *SH* surveys over the past decade. Current applications include the use of *SH*-waves to see through shallow gas accumulations (Harris et al., 2000) and in a downhole mode using accelerometers mounted on a cone penetrometer to record a VSP (Jarvis and Knight, 2000).

The target of near-surface reflection surveys often is only 1-2 boundaries (Baker, 1999) in contrast to the many horizons imaged at once on deeper reflection surveys. Even so, useful *P*-wave reflections may be difficult to obtain because the top of the saturated zone often presents a very large *P*-wave impedance contrast that masks reflections from deeper horizons. Moreover, the oblique rays illuminating shallow targets travel a very large part of their path in the "weathered layer." Consequently, the assumption that static delays are dependent only on station location may be unrealistic, making static correction difficult. Stacking fold is commonly low (six or less) due to the small recording systems often employed in near-surface surveys, and the optimal window (Hunter et al., 1984) over which reflections are clear cut may be narrow. As a result of these difficulties, a final *P*-wave reflection stack of near-surface data may result in lack of continuity and sharpness.

During the last several years, we have found that standard, 2-D acquisition and simple processing of *SH*-waves have been useful in shallow situations in which *P*-wave reflection exploration is ineffective. Figure 1 shows one such site, an old landfill near Norman, Oklahoma, from which a leachate plume has moved down gradient through alluvium toward a major river (Christenson et al., 1994). The underlying Hennessey shale, at a depth of approximately 10 m, prevents the leachate from migrating deeper into the earth.

The objective at an early stage in the study of this site was to obtain the detailed topography of the interface between the alluvium and the shale bedrock. We first obtained a low-resolution, velocity-depth model from *P*- and *SH*-wave refractions, and this model then guided design and processing of an *SH* reflection survey (Figure 1). The linearity of first arrivals suggested that to a first approximation, vertical velocity gradients are small; thus, constant velocity layers can be used in refraction inversion. Also, because the heterogeneous nature of the alluvium and the absence of laterally continuous clay lenses within the sands suggested that an isotropic model would suffice, effects of transverse isotropy were not included in the analysis.

A *P*-wave walkaway survey at the landfill showed a very short crossover distance beyond which a single first-arrival branch persists across the record (Figure 2). A subsequent delay-time survey, perpendicular to the walkaway, was conducted to record reversed refraction arrivals (Figure 1). Each pair of arrivals (Figure 3a) was mapped independently to the refractor by the conventional reciprocal method (Palmer, 1980; Burger, 1992). The refractor, which occurs at a depth of 1-2.5 m (Figure 3b), is the top of the water table.

An *SH*-wave walkaway survey (Figure 4) was conducted at the same location as the *P*-wave. Because the water table is transparent to the *SH*-refraction, the associated delay time survey (Figure 5) generates a refraction at the boundary between the alluvium and the shale. This occurs at a depth of approximately 9-10 m in good agreement with values determined by the USGS (Hasbrouck, 1997) in a similar refraction survey.

Figure 2 shows that a *P*-wave reflection from the top of the shale would be lost in ground roll and would be nearly coincident in time with other events. Frequency filtering using a high, low-cut frequency (Steeples et al., 1997) is not effective in improving the visibility of *P*-wave reflections on this record. The *SH*-wave reflection (Figure 4), on the other hand, is distinct in arrival time from other events and is undisturbed by Love waves in the optimal window. Ray-trace modeling using the program GX II (GX Technology, Houston) confirmed the identity of the *SH* reflection from the top of the shale (Hoyos et al., 1998).

Soil borings at the Norman landfill commonly encounter a gravelly interval several feet thick at the base of the alluvium, and this zone is associated with high hydraulic conductivity (Scholl and Christenson, 1998). Our *SH*-refraction survey is unlikely to have seen this interval for two reasons: (1) If velocity decreases in the gravel, then a refraction will not exist, or (2) if the gravel velocity exceeds that of the shale, a refraction can exist, but it may never be a first arrival because it follows a path that is slower than the path along the shale. If the gravel layer exists, therefore, it would be a blind zone (Burger, 1992) to *SH* refractions. Our recognition of reflection energy on the *SH* walkaway led us to conduct an *SH*-wave CMP reflection survey to image the top of the shale, and in the process, to search for a thin gravel layer resting on the shale.

An *SH*-wave reflection line (Figure 1) using off-end geometry employed a single, transversely directed sledgehammer blow as source at stations spaced .3 m apart for a line length of 47 m. Nominal fold was 4. A Strataview (Geometrics) 24 channel system recorded single, 10-Hz, transversely oriented geophones at a sample rate of .5 ms. Figure 6 shows acquisition. Processing used the PC package, Seistrix 3 (Interpex). Table 1 shows the processing flow.

Figure 7a shows representative shot gathers before pro-

Table 1. Processing flow for *SH* reflection data

1. Assign geometry
2. Sort
3. Edit
4. Band-pass filter (2-5-200-400), zero phase
5. Edit
6. F-K filter
Positive K plane: pass above 272 m/s; 24 db/octave slope
Negative K plane: pass above 272 m/s; 24 db/octave slope
7. Normal moveout
Stretch mute 130%
8. CMP-consistent residual statics
Pilot 12 CMPs
Correlation window 12-255 ms
Maximum shift 5 ms
9. Analysis
10. CMP stack
11. Depth conversion
100% of smoothed stacking velocities

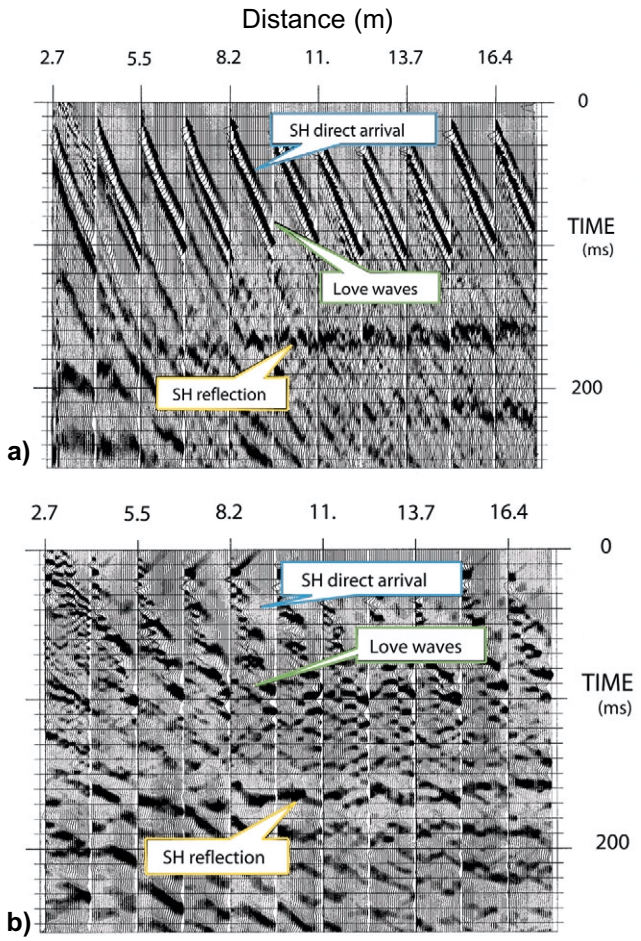

Figure 7. Representative shot gathers at the start of the line. (a) The *SH* reflection is broken into segments by the strong Love waves, which have approximately the same moveout as the *SH* direct arrival. (b) Band-pass and *f-k* filtered shot gathers after NMO and residual statics correction. The continuity of the *SH* reflection is restored.

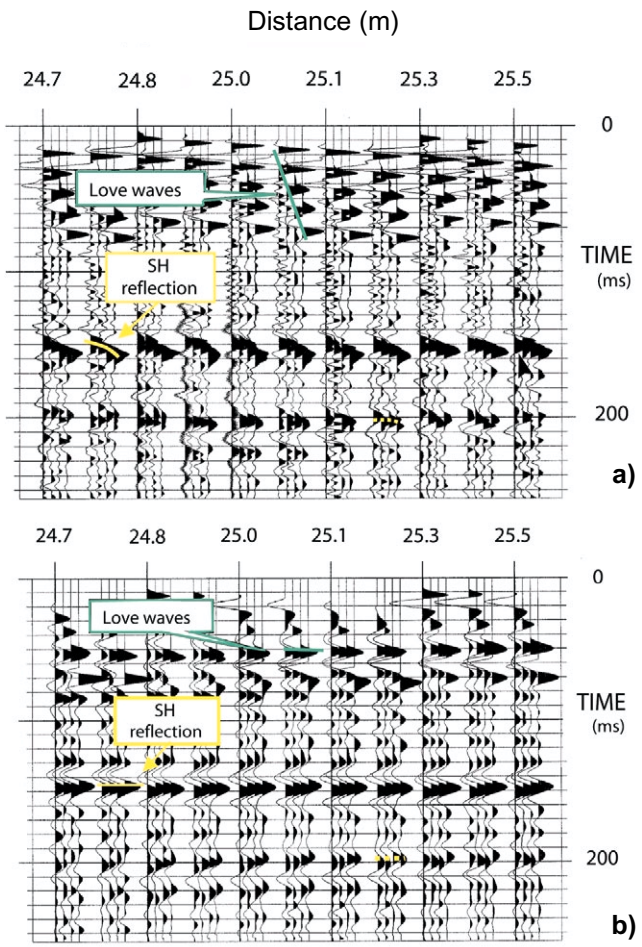

Figure 8. Representative CMP gathers in the middle of the line. (a) Low-frequency, slow Love waves (green) dominate the CMP gathers to approximately 80 ms. A strong *SH* reflection (yellow) at 150 ms exhibits good continuity, and a less consistent event (dashed yellow) at 200 ms may also be a reflection. High-frequency (150-200 Hz) events between 90 and 150 ms are discontinuous. (b) After band-pass and FK filtering and residual static correction, the NMO-corrected *SH* reflection is distinct and flattened. Event continuity from 80 to 150 ms has been improved. Filtering partially attenuates the Love waves, but after NMO correction, the Love waves line up, masquerading as reflections. This suggests caution in interpreting the stacked section at times less than 90 ms.

cessing. Strong Love waves interfere with the direct arrival and break up the *SH* reflection at approximately 160 ms. After filtering, NMO correction, and residual statics correction, the continuity of the reflection is improved (Figure 7b). A corresponding improvement is seen after processing of representative CMP gathers (Figure 8). Velocity spectra typically show a distinct bull's eye (Figure 9) at approximately 160 ms and 125 m/s. This velocity represents the average velocity through the alluvium and is similar in value to the direct-arrival velocity of 122 m/s (SH walkaway, Figure 4) and 137 m/s (*SH* delay-time survey, Figure 5), respectively. Bachrach et al. (1998) also report a good correspondence between refraction- and reflection-derived velocities in unconsolidated sand.

The stacked, depth-converted section (Figure 10) shows a strong, continuous reflection from the base of the alluvium at a depth of approximately 9 m, in agreement with the delay-time result (Figure 5b). Depressions in the surface of the shale are interpreted to be channels, and the higher frequency reflection above the channel at a distance of 10 m may be the top of a gravel lens filling the channel. The thickness of this lens is approximately 1 m. Water wells at other sites in the Canadian River floodplain are reported to produce from a coarse gravel layer several feet thick. Taking the gravel velocity equal to the derived rms velocity (125 m/s) and estimating a predominant frequency of 67 Hz, the 1/4 wavelength thickness of the gravel lens would be .47 m. This suggests that a thin layer such as that reported by well owners and inferred in Figure 10 would indeed be resolved by the present *SH*-wave survey.

The reflection line is tied by a borehole, MLS 54, at its northern end (Figure 1). Although the fold of the survey is low near the borehole and the stacked image is irregular, the reflection at 10 m (Figure 10) agrees closely with the depth to the top of the Hennessey shale from coring (Figure 11). A seismic zone with a distinct reflection at 5.9 m (Figure 10) may correlate with the zone of thin clay lenses encountered at 5.2 m (Figure 11).

Poisson's ratio values from the walkaway surveys and

delay-time surveys are .40 and .43, respectively, and the corresponding V_P/V_S ratios are 2.4 and 2.79. Ratios of this magnitude for unconsolidated sediments of sand/clay lithology have been reported elsewhere (e.g., 3.6 on average for glacial deposits; Carr et al., 1998). Slug tests at several wells (Scholl and Christenson, 1998) have established the hydraulic conductivity as a function of depth (Figure 12). The greatly decreased hydraulic conductivity at a depth of approximately 5.5 m in wells MLS 54 and 80 correlates closely with a distinct zone of seismic reflections at 5.9 m (Figure 10) and the presence of a zone with thin clay lenses at a depth of 5.2 m (Figure 11).

Conclusions. The simple, near-surface *SH* study presented here reveals a shale boundary incised by channels that are possibly filled by gravel lenses, approximately 1 m in thick-

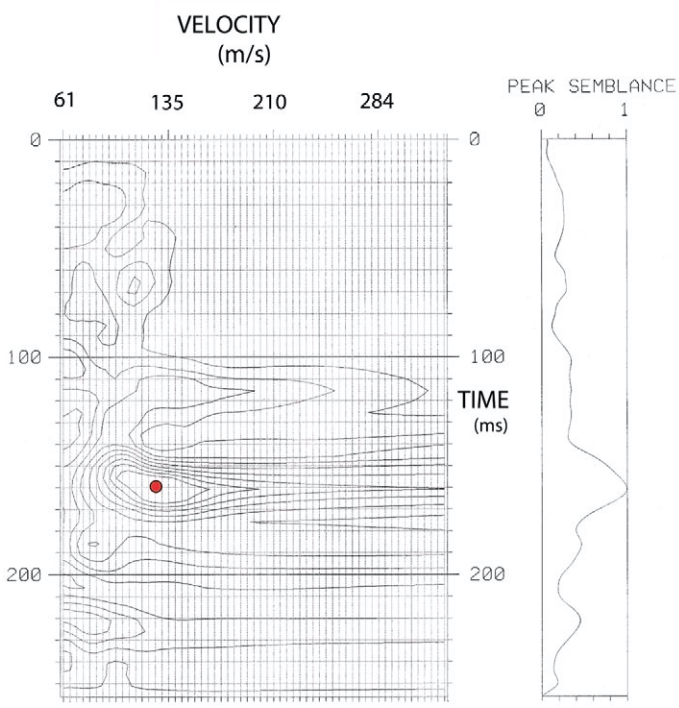

Figure 9. The semblance map for a CMP in the middle of the line shows a distinct bull's-eye at a moveout velocity of 134 m/s and a time of 160 ms.

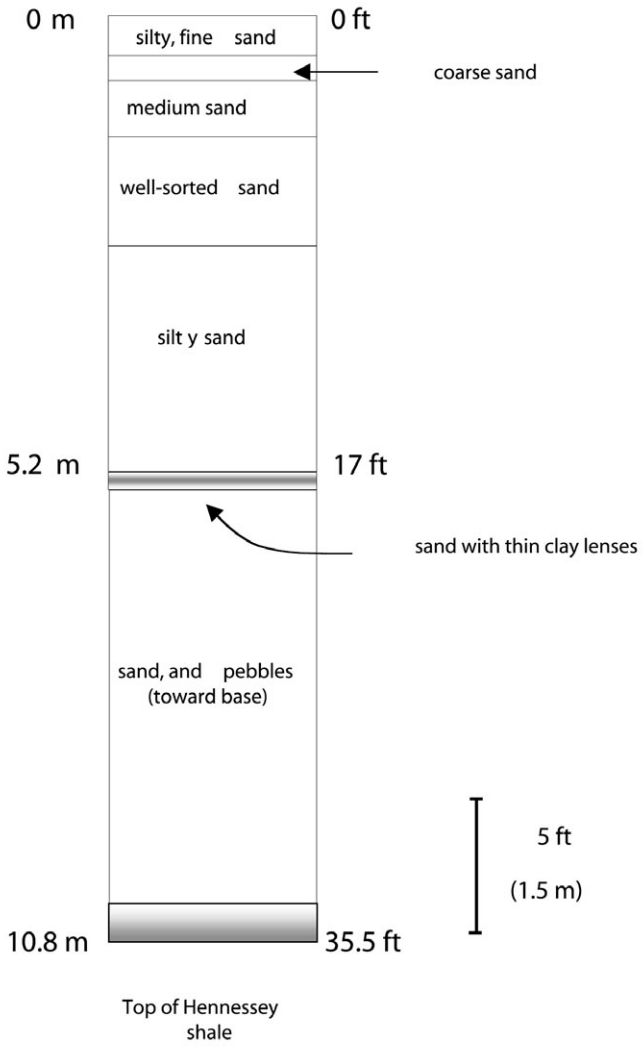

Figure 11. Stratigraphic log from MLS 54, a borehole at the origin of the reflection survey (Figure 1). It shows a zone of sand and thin clay lenses at a depth of 5.2 m. The top of the Hennessey shale occurs at 10.8 m (after Scholl and Christenson, 1998).

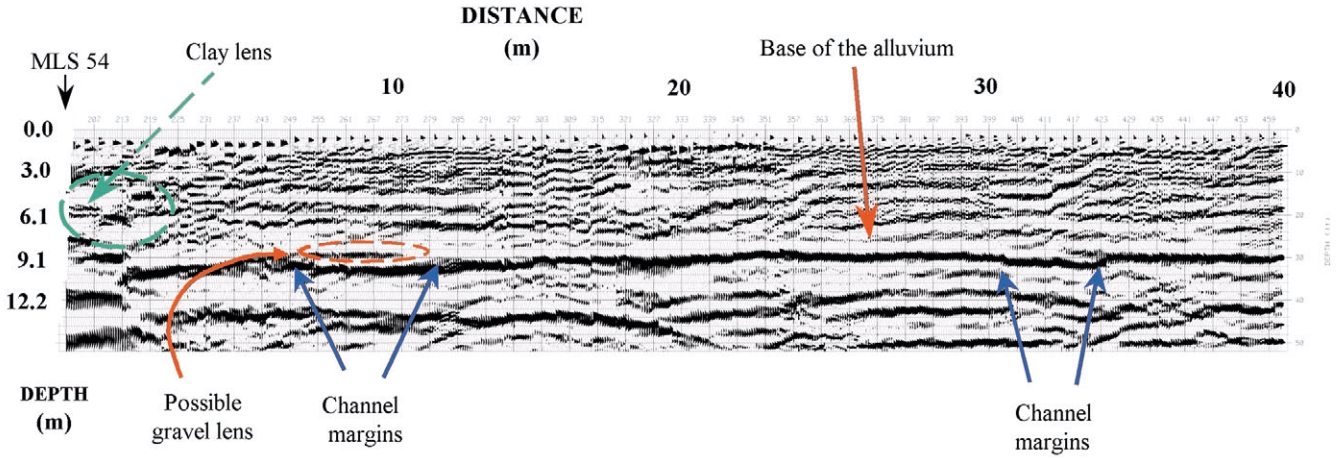

Figure 10. Depth-converted *SH*-wave, stacked section. The top of the shale at a depth of approximately 9 m is very clear cut. Depressions in the top of the shale are interpreted to be channels, possibly filled with a gravel lens (CMP 255-275). Reflections from a depth of 6 m correlate with the presence of clay lenses in borehole MLS 54.

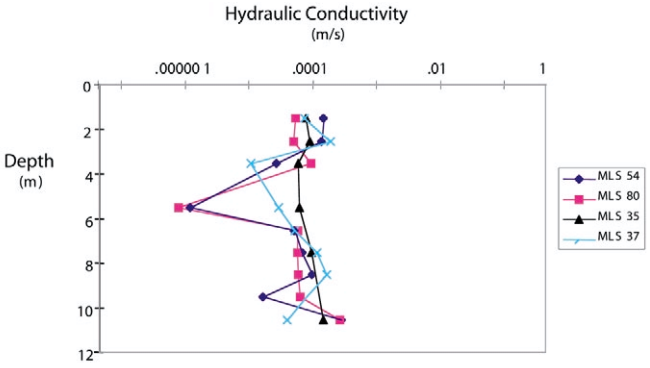

Figure 12. A decrease in hydraulic conductivity at a depth of approximately 5.5 m correlates with the zone of sand with thin clay lenses observed in the stratigraphic log (from Scholl and Christenson, 1998).

ness. These features could not be seen on *P*-wave records even after processing. The great interpretational advantage of *SH*-waves is that the slow shear-wave velocities spread reflections out in time, and Love wave interference lies outside the optimal reflection window. *P*- and *SH*-wave refractions, when used together, can be used to define an initial velocity model and control placement of a reflection spread.

Many successful near-surface *SH* reflection surveys during the 1990s have been fostered by earlier developments in the energy industry. The expertise now being practiced by near-surface geophysicists may in turn return new approaches to seismic explorationists.

Suggested reading. "High-resolution shallow-seismic experiments in sand, Part II: Velocities in shallow unconsolidated sand" by Bachrach et al. (GEOPHYSICS, 1998). *Processing Near-Surface Seismic-Reflection data: A Primer* by Baker (SEG Course Notes 9, 1999). *Exploration Geophysics of the Shallow Subsurface* by Burger (Prentice-Hall, 1992). *Norman Landfill Research Plan* by Christenson et al. (USGS provisional draft, 1994). *Near-Field Seismic Study Near Norman, Oklahoma Landfill* by Hasbrouck (USGS draft report, 1997). "Seismic shear-wave surveys at the Norman Landfill Site" by Hoyos et al. (Oklahoma Geology Notes, Oklahoma Geological Survey, 1998). "Shallow seismic reflection mapping of the overburden-bedrock interface with the engineering seismograph—some simple techniques" by Hunter et al. (GEOPHYSICS, 1984). *The Generalized Reciprocal Method of Seismic Refraction Interpretation* by Palmer (SEG, 1980). *Spatial Variability in Hydraulic Conductivity Determined by Slug Tests in the Canadian River Alluvium Near the Norman Landfill, Norman, Oklahoma* by Scholl and Christensen (USGS Water Resources Investigations Report 97-4292, 1998). "A workshop examination of shallow seismic reflection surveying" by Steeples et al. (*TLE*, 1997). "Shear data in the presence of azimuthal anisotropy" by Alford (SEG 1986 *Expanded Abstracts*). "Shallow *SH*-refraction survey on Mexico City mud: amplification by wedge effects" by Alvarez et al. (*First Break*, 1995). "Shear-wave studies in glacial till" by Carr et al. (GEOPHYSICS, 1998). "Shear-wave technology in petroleum exploration—past, current, and future" by Domenico and Danbom (in *Shear-wave Exploration*, SEG, 1987). *Vertical Seismic Profiling* by Gal'perin (SEG, 1974). "Two-component acquisition as a routine procedure" by Garotta (in *Shear-wave Exploration*, SEG, 1987). "Seismic reflection investigations of a bedrock surface buried under alluvium" by Goforth and Hayward (GEOPHYSICS, 1992). "Near-surface reflection surveys in the Frazer River delta, B.C., Canada" by Harris et al. (SEG 2000 *Expanded Abstracts*). "Four shallow-depth, shear-wave feasibility studies" by Hasbrouck (GEOPHYSICS, 1991). "Near-surface VSP surveys using the seismic cone penetrometer" by Jarvis and Knight (GEOPHYSICS, 2000). "Correlation between *P*-wave AVOA and *S*-wave traveltime anisotropy in a naturally fractured gas reservoir" by Lynn et al. (*TLE*, 1996). "Shear wave analysis for azimuthal anisotropy using pseudorotation of marine VSP" by MacBeth (EAGE 1996 *Extended Abstracts*). "A 9-C–2-D land experiment for lithology estimation of a Permian clastic reservoir" by Macrides and Kelamis (*TLE*, 2000). "Effects of near-surface waveguides on shallow high-resolution refraction and reflection data" by Robertsson et al. (*Geophysical Research Letters*, 1996). "Case history: 3-D shear-wave processing and interpretation in radial-transverse (*SV-SH*) coordinates: by Simmons et al. (SEG 1999 *Expanded Abstracts*). *Multicomponent Seismology in Petroleum Exploration* by Tatham and McCormack (SEG, 1991). TLE

Acknowledgments: We thank U.S Geological Survey personnel Scott Christenson (Oklahoma City) and Bill Hasbrouck (Denver) for access to the Norman landfill site and for assistance in improving our shear-wave source, respectively. Gary Hoover was instrumental in obtaining horizontal component geophones from Phillips Petroleum Company. J. Hoyos received financial support from National Science Foundation project OSR-9553363 at the University of Oklahoma.

Corresponding author: ryoung@ou.edu